ELSEVIER

Biophysical Chemistry 125 (2007) 471 – 482

Biophysical Chemistry

http://www.elsevier.com/locate/biophyschem

Volume and hydration changes of DNA–ligand interactions

Xuesong Shi, Robert B. Macgregor Jr. *

Leslie Dan Faculty of Pharmacy, University of Toronto, Canada

Received 29 August 2006; received in revised form 25 October 2006; accepted 25 October 2006
Available online 16 November 2006

Abstract

We report the volumetric and other thermodynamic properties of ethidium bromide (EB), propidium iodide (PI) and daunomycin (DAU) intercalating with poly(dA)•poly(dT), poly[d(A–T)]•poly[d(A–T)], and poly[d(G–C)]•poly[d(G–C)], respectively, as well as minor groove binder Hoechst 33258 binding with poly[d(A–T)]•poly[d(A–T)]. The data were obtained using fluorescence titration and hydrostatic pressure measurements. Our thermodynamic data are combined with enthalpies from literature reports to analyze the thermodynamic characteristics of the different interactions. The differences are interpreted based on three processes related to hydration: I. burial of non-polar hydrophobic solvent accessible surface, II. burial of polar surface and formation of solute–solute H-bonds, and III. disruption of "structural" hydration. Sequence dependent conformational changes may also be important when comparing ligand binding to different DNA sequences. We conclude that a combination of different thermodynamic parameters, especially volume change, is essential in order to understand the role of hydration in the energetics of DNA–ligand interactions.

Keywords: DNA–ligand interactions; Volumetric parameters; Binding parameters; Hydration; Hydrostatic pressure

1. Introduction

Changes in hydration play an essential role in the thermodynamics of the non-covalent interactions formed by biological molecules. However, despite being the target of great interest, the quantitative understanding of the contribution of hydration to the energetics of a non-covalent complex remains elusive. One practical consequence of the lack of understanding is that modelling hydration is a major obstacle in computer-assisted drug design. The major impediment to the characterization of hydration arises from the fact that the actual process of water interacting with one or more solutes takes place amid a background of interactions between water molecules interacting with each other. The water–water interactions are usually similar to the water–solute interactions. Changes in solvent accessible surface of the solute, either in area, or physical properties, such as charge, polarity, or shape, can influence solute–water interactions. Adding to the difficulty of quantitatively assessing the role played by hydration in the thermodynamics of non-covalent complexes is the paucity of comparable experimental results.

Among water–solute interactions, the hydrophobic interaction is perhaps the closest to being quantified. The free energy arising from the hydrophobic hydration has been empirically linked to heat capacity change: $\Delta G_{hyd,np}=(80\pm10)\Delta C_p$ [1,2] and later to solvent accessible surface area ΔA through empirical relationships between ΔC_p and ΔA [3,4]. However, the relationship proposed by Spolar et al. [1] requires that most of the solvent accessible surface lost upon formation of the complex be hydrophobic. This situation is rarely the case for DNA–ligand complexes. Recent attempts to dissect the free energy of DNA–ligand interactions [3,5–7] have recognized the importance of hydration.

The volumetric parameters are more directly related to hydration than free energy or enthalpy. Hydration changes, arising from the release of hydration water into bulk and changes in solvent accessible surface are the sources of most of the volumetric changes during DNA–ligand interactions. In contrast, hydration change is only one of several factors that comprise ΔG, ΔH, and ΔS. The direct relationship between hydration and volumetric properties makes volumetric methods ideal for studying hydration; this is well recognized in reviews of DNA hydration [8]. Unfortunately, volumetric data describing DNA–ligand interactions are still scarce and

* Corresponding author. Department of Pharmaceutical Sciences, Leslie Dan Faculty of Pharmacy, University of Toronto, 144 College Street, Toronto, Ontario, Canada M5S 3M2. Tel.: +1 416 978 7332; fax: +1 416 978 8511.
E-mail address: rob.macgregor@utoronto.ca (R.B. Macgregor).

0301-4622/$ - see front matter © 2006 Elsevier B.V. All rights reserved.
doi:10.1016/j.bpc.2006.10.011

not very systematic. Most of the volume changes were measured by either densimetric methods or measuring pressure dependence of the association constant, K_a. The interaction of ethidium bromide (EB), propidium iodide (PI) [9] and Hoechst33258 [10,11] with AT-containing polymers have been studied by pressure methods. Densimetric methods have been used to study the volumetric properties of the complexes formed by EB [12], Distamycin [13], and netropsin [14,15] with synthetic DNA polymers. It remains difficult to broadly assess the role of hydration in these complexes because most of the studies have been performed under a limited range of experimental conditions.

In this work, we present volumetric data for the interaction of the intercalators EB, PI, and daunomycin binding with poly (dA)•poly(dT), poly[d(A–T)]•poly[d(A–T)] and poly[d(G–C)] •poly[d(G–C)] and the minor groove binder Hoechst 33258 complexed with poly[d(A–T)]•poly[d(A–T)]. Combining our volumetric and free energy data with literature values for ΔH and deduced ΔS gives us a better understanding of DNA–ligand interactions, especially the role of hydration effect, through a systemic comparison of different DNA–ligand binding combinations.

2. Materials and methods

2.1. Materials

Ethidium bromide (EB), propidium iodide (PI), daunomycin (DAU) and Hoechst 33258 were obtained from Sigma-Aldrich Co. and used without further purification. The synthetic polymers, poly(dA)•poly(dT), poly[d(A–T)]•poly[d(A–T)] and poly[d(G–C)]•poly[d(G–C)] were purchased from Amersham Biosciences Corporation. The DNA polymers were dissolved in buffer, and then dialyzed against the same buffer. The concentrations of stock DNA and ligand solutions were determined spectrophotometrically using molar extinction coefficients: ϵ_{259}=12,000 M^{-1} cm^{-1} for poly(dA)•poly(dT) [16], ϵ_{262}=13,200 M^{-1} cm^{-1} for poly[d(A–T)]•poly[d(A–T)] [17], ϵ_{255}=16,800 for poly[d(G–C)]•poly[d(G–C)] [18], ϵ_{480}=5800 M^{-1} cm^{-1} for EB [19], ϵ_{493}=5900 M^{-1} cm^{-1}. For PI [20], ϵ_{480}=11,500 M^{-1} cm^{-1} for DAU [21] and ϵ_{338}=42,000 M^{-1} cm^{-1} Hoechst 33258 [22], respectively. The concentration of DNA polymers is expressed in moles of base pairs. All measurements were preformed in buffer solutions consisting of 20 mM Tris–HCl, pH 7.2, 0.1 mM EDTA and the desired amount of NaCl.

2.2. Fluorometric titrations

Fluorescence titrations were performed on a Spex FluoroMax 3 spectrofluorometer (Jobin Yvon, Inc., Edison, NJ) at room temperature to determine the equilibrium binding parameters of ligands binding with DNA. DNA solutions were titrated with concentrated ligand solutions. The excitation and emission wavelengths were 512 nm and 600 nm, respectively, for EB titration; 526 nm and 610 nm, respectively, for PI titration; 480 nm and 555 nm, respectively, for DAU titration; 355 nm and 467 nm, respectively, for Hoechst 33258 titration. Data sets consisting of binding density, r=[bound EB]/[total DNA base pairs], and [L], the concentration of unbound EB, were determined from the titration. Then the data of r and [L] were analyzed with site-exclusion model [23]:

$$\frac{r}{[L]} = K_a(1-nr) \times \left[\frac{(2\omega-1)(1-nr)+r-R}{2(\omega-1)(1-nr)}\right]^{n-1}\left[\frac{1-(n+1)r+R}{2(1-nr)}\right]^2$$

$$R = \{[1-(n+1)r]^2 + 4\omega r(1-nr)\}^{1/2}$$

in which K_a is the equilibrium binding constant, n is the size of the binding site in base pairs, and ω is a cooperativity parameter. K_a, n, and ω were determined by nonlinear fitting using Origin (OriginLab Corp., Northampton, MA) with n restricted to be an integer according to the original excluded-site model. The restriction of n to integer values was also important because n and ω are highly correlated [24] and it is nearly statistically impossible to fit both without some constrains. Similar to other studies of the binding parameters of these ligands, the fluorescence properties of bound ligands are assumed to be independent of binding density r.

2.3. High-pressure fluorescence measurements

Based on the standard thermodynamic relationship: $(\partial \ln K_a/\partial P)_T = -\Delta V^\circ/RT$, where R is the gas constant, the molar volume change of DNA–ligand binding was determined though measuring the pressure dependence on binding constants. The change of binding affinity with pressure was measured using a Fluoromax 3 spectrofluorometer. A more detailed description can be found in our previous publications [25]. The pressure dependence of $\ln K_a$ was fitted with second order polynomial using Origin (OriginLab Corp., Northampton, MA) to obtain ΔV and its pressure derivative, the isothermal compressibility.

3. Results

3.1. Binding parameters

We report the equilibrium parameters of ten DNA–ligand systems: the intercalators EB, PI, and DAU with poly[d(A–T)]• poly[d(A–T)], poly(dA)•poly(dT) and poly[d(G–C)]•poly[d (G–C)] and minor groove binder Hoechst 33258 with poly[d (A–T)]•poly[d(A–T)]. The data were obtained from fluorescence titration measurements. For each ligand–DNA system, titrations were performed at four or five different NaCl concentrations ranging from 25 to 220 mM. The results are summarized in Table 1. The equilibrium constant, K_a, of solution with 50 mM added NaCl and corresponding free energy, ΔG, are listed for comparison between different systems. No statistically significant salt dependence was observed for the cooperativity, ω, or the binding size, n. At the same NaCl concentration, the typical error in K_a, and the cooperativity, ω, is about 10%; the corresponding error of ΔG is 0.06 kcal/mol. The error reported in Table 1 for ω is the standard deviation of ω at different salt concentrations.

The ligands can be divided into three categories: EB and PI are structurally similar intercalators; however, ethidium is a

Table 1
Binding parameters

	n	ω	K_a^a ($\times 10^6$ M^{-1})	ΔG^a (kcal/mol)
EB binding with				
poly(dA)•poly(dT)	3	1.9±0.6	0.037	−6.2
poly[d(A–T)]•poly[d(A–T)]	2	0.8±0.1	0.89	−8.1
poly[d(G–C)]•poly[d(G–C)]	2	1.1±0.3	0.27	−7.4
PI binding with				
poly(dA)•poly(dT)	4	1.4±0.5	0.51	−7.8
poly[d(A–T)]•poly[d(A–T)]	3–4	1.6±0.6	5.6	−9.2
poly[d(G–C)]•poly[d(G–C)]	2	0.7±0.6	4.8	−9.1
DAU binding with				
poly(dA)•poly(dT)	1	7±5	0.082	−6.7
poly[d(A–T)]•poly[d(A–T)]	1–2	0.8±0.6	3.3	−8.9
poly[d(G–C)]•poly[d(G–C)]	1–2	0.5±0.1	2.4	−8.7
Hoechst 33258 binding with				
poly[d(A–T)]•poly[d(A–T)]	6–7	5±2	19.3	−9.9

[a] In 50 mM NaCl, 20 mM Tris–HCl, pH 7.2.

monocation and propidium is a dication; DAU is an intercalator with a flexible sugar ring that occupies the minor groove of DNA; and finally, Hoechst 33258 binds to the DNA minor groove.

3.1.1. Ethidium bromide and propidium iodide

EB intercalation with poly[d(A–T)]•poly[d(A–T)] and poly[d(G–C)]•poly[d(G–C)] share similar binding parameters, in both cases the ligand occupies two base pairs and the binding displays no significant cooperativity. The equilibrium constant for EB binding with poly[d(A–T)]•poly[d(A–T)] is approximately three times larger that that for the binding with poly[d(G–C)]•poly[d(G–C)]. On the other hand, the complex formed with poly(dA)•poly(dT) has a larger binding site size (n=3), displays cooperativity, and the value of K_a is 24±3 fold less than that of poly[d(A–T)]•poly[d(A–T)]. The affinity of PI for poly(dA)•poly(dT) and poly[d(A–T)]•poly[d(A–T)] differs only by a factor of approximately 11±2 and PI binding to these two polymers has similar values of n and ω. PI exhibits similar binding affinity to poly[d(G–C)]•poly[d(G–C)] and poly[d(A–T)]•poly[d(A–T)] but with a smaller values of n and ω. No statistically significant cooperativity was observed for PI binding with these three polymers. Binding with PI generally influences more base pairs (larger n) and has a higher affinity than EB at moderate salt concentrations. The binding parameters obtained (n, ω and K_a) are in good agreement with literature reports [9,16,26,27]. Neither n nor ω of EB binding with poly[d(G–C)]•poly[d(G–C)] have been reported in the literature.

3.1.2. Daunomycin

In a manner similar to EB, the equilibrium parameters describing the complex formed between DAU and poly(dA)•poly(dT) differ significantly from those of the other two polymers. The value of K_a for the interaction with this polymer is 40-fold smaller than that for binding with poly[d(A–T)]•poly[d(A–T)]. Binding of DAU with poly[d(A–T)]•poly[d(A–T)] and poly[d(G–C)]•poly[d(G–C)] exhibit essentially the same affinity. For all three polymers, the value of the excluded site parameter is small (n=1 to 2). Cooperative, non-cooperative, and anti-cooperative binding were observed for poly(dA)•poly(dT), poly[d(A–T)]•poly[d(A–T)] and poly[d(G–C)]•poly[d(G–C)], respectively. The K_a values we measured are in good agreement with literature results obtained under similar experimental conditions [21,28–32]. In the literature, the size of the binding site, n, ranges from 2 to 3 for poly[d(A–T)]•poly[d(A–T)] and poly[d(G–C)]•poly[d(G–C)] and 1 to 2 for poly(dA)•poly(dT) [21,28,29,31,32], which is similar to our results. None of the literature studies have considered the potential cooperativity of the binding and it might be part of the reason for the difference between the value of n we observed and those reported in the literature.

3.1.3. Hoechst 33258

Hoechst 33258 binds with poly[d(A–T)]•poly[d(A–T)] with positive cooperativity and occupies 6 to 7 base pairs. The binding

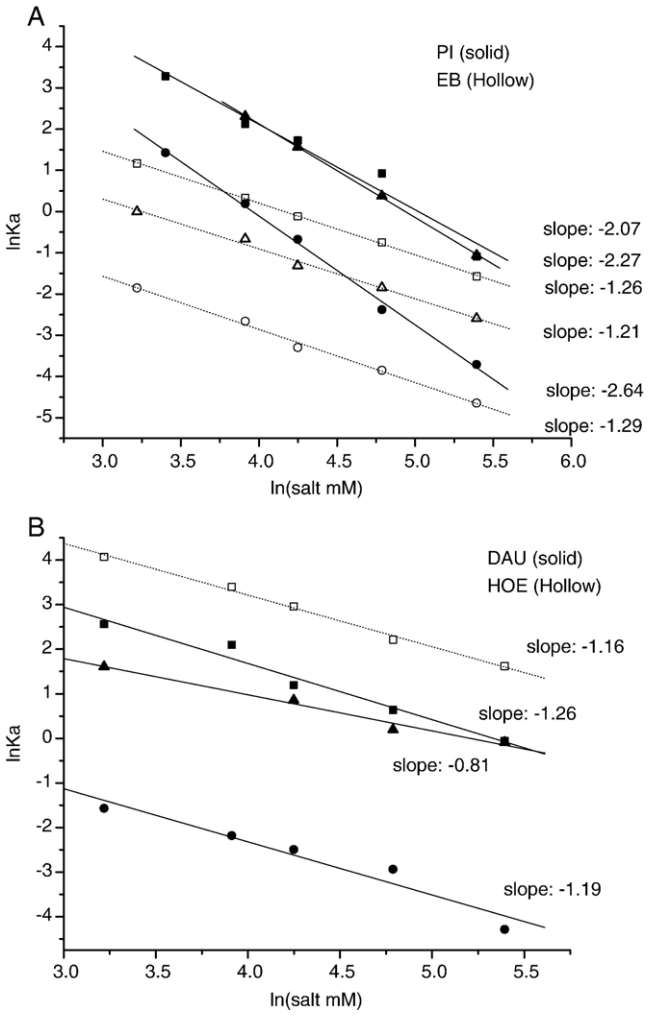

Fig. 1. A. Salt dependence of equilibrium constant, K_a, of EB and PI binding with DNA. B. Salt dependence of equilibrium constant, K_a, of DAU and Hoechst 33258 binding with DNA. Unit of K_a is μM^{-1}. The circles are data for poly(dA)•poly(dT). The squares are for poly[d(A–T)]•poly[d(A–T)] and the triangles are data for poly[d(G–C)]•poly[d(G–C)].

Table 2
Salt dependence of binding affinity

	Charge of ligand	ΔG^a (kcal/mol)	$-d\ln K_a/d\ln[salt]$	ΔG_{other} (kcal/mol)
EB binding with				
poly(dA)•poly(dT)	+1	−6.2	1.29±0.05	−4.3±0.2
poly[d(A–T)]•poly[d(A–T)]	+1	−8.1	1.26±0.02	−6.1±0.1
poly[d(G–C)]•poly[d(G–C)]	+1	−7.4	1.21±0.06	−5.6±0.3
PI binding with				
poly(dA)•poly(dT)	+2	−7.8	2.64±0.09	−3.6±0.4
poly[d(A–T)]•poly[d(A–T)]	+2	−9.2	2.07±0.22	−5.9±1.1
poly[d(G–C)]•poly[d(G–C)]	+2	−9.1	2.27±0.03	−5.5±0.2
DAU binding with				
poly(dA)•poly(dT)	+1	−6.7	1.19±0.17	−4.8±0.8
poly[d(A–T)]•poly[d(A–T)]	+1	−8.9	1.26±0.13	−7.0±0.6
poly[d(G–C)]•poly[d(G–C)]	+1	−8.7	0.81±0.08	−7.4±0.4
Hoechst 33258 binding with				
poly[d(A–T)]•poly[d(A–T)]	+1	−9.9	1.16±0.05	−8.1±0.2

[a] Corresponding to the measurements in 50 mM NaCl, 20 mM Tris–HCl, pH 7.2.

constant is larger than that of the three intercalators, which is expected for a minor groove binder. The binding site size n is in good agreement with the value reported by Loontiens et al., $n=5$–6 [22]. The experimentally observed positive cooperativity has also been implied by an NMR study [33]. The strong binding affinity is also in good agreement with literature reports [22,34].

3.2. Salt dependence of binding affinity

The salt dependence of K_a for the ten binding systems is plotted in Fig. 1 and the results are summarized in Table 2. The binding constant, K_a, decreases with increasing salt concentration for all systems studied (Fig. 1). This behaviour arises from the release of counter-ions upon binding with a positively charged ligand [35–37]. The change of DNA conformation upon binding, such as unwinding, also can lead to counter-ion release to a lesser extent. The value of the slope, $-d\ln K_a/d\ln[salt]$, is proportional to the number of counter-ions released upon binding. As seen in Table 2, the values of $-d\ln K_a/d\ln[salt]$ are close to unity for the monovalent cations EB, DAU and Hoechst 33258 and close to 2 for the divalent cation PI, as expected. However PI binding with poly(dA)•poly(dT) has a significantly higher $-d\ln K_a/d\ln[salt]$ than the other two polymers and DAU binding with poly[d(G–C)]•poly[d(G–C)] has a smaller value of $-d\ln K_a/d\ln[salt]$ than the other monovalent ligands.

By extrapolating the values of the free energy measured at lower salt concentrations to 1 M, the electrostatic or polyelectrolyte free energy, $\Delta G_{pe}=-(d\ln K_a/d\ln[salt])RT\ln[salt]$, approaches zero [36]. This allowed us to calculate $\Delta G_{1M}=\Delta G_{other}$ the free energy that arises from non-electrostatic contributions. The values are shown in Table 2. The magnitude of the non-electrostatic component of the binding free energy (ΔG_{other}) is roughly in the order: Hoechst 33258 > daunomycin > EB ≈ PI and poly[d(G–C)]•poly[d(G–C)] ≈ poly[d(A–T)]•poly[d(A–T)] > poly(dA)•poly(dT). It is noteworthy that the difference in the binding affinity of EB and PI at moderate salt concentration is mostly electrostatic in origin.

3.3. Volumetric change associated with binding

The molar volume change and molar isothermal compressibility change associated with binding at different salt concentrations were obtained by monitoring the fluorescence as a function of pressure. The dependencies of the molar volume changes (ΔV) on the salt concentration are plotted in Fig. 2. From this Figure, it appears that there is no strong salt dependence of ΔV for the systems we have studied; this is also true for the change in compressibility. The volumetric data are summarized in Table 3.

Although generally we did not observe a strong salt dependence, the binding of PI with poly[d(G–C)]•poly[d(G–C)] and DAU with poly[d(A–T)]•poly[d(A–T)] displayed a noticeable decrease in ΔV with increasing salt concentration. These trends

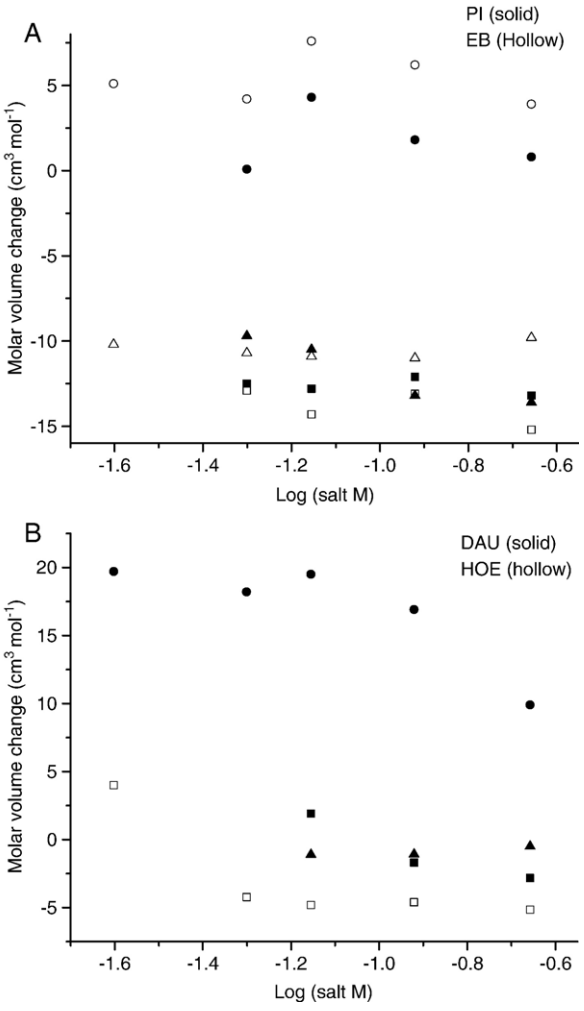

Fig. 2. A. Salt dependence of molar volume change of EB and PI binding with DNA. B. Salt dependence of molar volume change of DAU and Hoechst 33258 binding with DNA. The circles are data for poly(dA)•poly(dT). The squares are data for poly[d(A–T)]•poly[d(A–T)] and the triangles are data for poly[d(G–C)]•poly[d(G–C)].

Table 3
Molar volume change and compressibility change of binding at 25 °C

	ΔV (cm^3/mol)[a]	$\Delta\kappa_T$ (10^{-3} cm^3 mol^{-1} MPa^{-1})[a]
EB binding with		
poly(dA)•poly(dT)	5.4±0.3	−5±3
poly[d(A–T)]•poly[d(A–T)]	−13.9±0.2	−17±1
poly[d(G–C)]•poly[d(G–C)]	−10.5±0.1	−22±1
PI binding with		
poly(dA)•poly(dT)	1.7±0.2	−31±1
poly[d(A–T)]•poly[d(A–T)]	−12.7±0.1	−26±1
poly[d(G–C)]•poly[d(G–C)]	−11.8±0.2	−20±2
DAU binding with		
poly(dA)•poly(dT)	16.8±0.2	61±2
poly[d(A–T)]•poly[d(A–T)]	−0.9±0.3	23±3
poly[d(G–C)]•poly[d(G–C)]	−0.9±0.2	−24±2
Hoechst 33258 binding with		
poly[d(A–T)]•poly[d(A–T)]	−3±0.3	−15±2

[a] Average of values from different salt concentrations.

have also been observed for all interactions with poly(dA)•poly(dT) at moderate to high salt concentrations (70 mM to 220 mM).

The ten systems studied possess a large range of values of the associated volumetric parameters, including both positive and negative ΔV and compressibility changes. Complexes formed with poly(dA)•poly(dT) generally have values of ΔV that are more positive than those of the other two polymers. The difference of ΔV of binding with poly(dA)•poly(dT) and the average of ΔV of binding with poly[d(A–T)]•poly[d(A–T)] and poly[d(G–C)]•poly[d(G–C)] (i.e. the $\Delta\Delta V$) are very similar for EB, PI and DAU at 17.8, 14.0 and 17.7 cm^3/mol, respectively. In contrast to these values, the ΔV of binding with poly[d(A–T)]•poly[d(A–T)] and poly[d(G–C)]•poly[d(G–C)] are more similar, with $\Delta\Delta V$ values of 3.4, −0.9 and 0.0 cm^3/mol for EB, PI and DAU, respectively. The overall ΔV patterns are similar for EB and PI, the differences in ΔV for EB and PI binding with poly(dA)•poly(dT), poly[d(A–T)]•poly[d(A–T)] and poly[d(G–C)]•poly[d(G–C)] are small, +3.7, −1.2 and +1.3 cm^3/mol, respectively. The values of ΔV for the binding of DAU parallel those observed for EB and PI although they are more positive, with average change of 13.2, 12.4 and 10.3 cm^3/mol for binding with poly(dA)•poly(dT), poly[d(A–T)]•poly[d(A–T)] and poly[d(G–C)]•poly[d(G–C)], respectively. Binding of Hoechst 33258 with poly[d(A–T)]•poly[d(A–T)] has small negative ΔV of about −5 cm^3/mol for most of the salt range studied except at the lowest salt concentration of 25 mM it has a small positive ΔV of 4 cm^3/mol.

Most of the systems have negative compressibility changes with values approximately -20×10^{-3} cm^3 mol^{-1} MPa^{-1}, the range is −15 to -31×10^{-3} cm^3 mol^{-1} MPa^{-1}. The exceptions are DAU binding with two AT polymers, both have positive compressibility changes; and EB binding with poly(dA)•poly(dT), which has a negative compressibility change with a much smaller magnitude, -5×10^{-3} cm^3 mol^{-1} MPa^{-1}. Comparable values of the adiabatic compressibility have been reported on EB binding with poly[d(A–T)]•poly[d(A–T)] and poly[d(G–C)]•poly[d(G–C)] [12]. We are unaware of other compressibility data for these interactions in the literature.

3.4. Temperature dependence of volume changes of EB binding with poly[d(G–C)]•poly[d(G–C)]

In an earlier study [25], we measured the temperature dependence of volumetric changes of EB binding with poly(dA)•poly(dT) and poly[d(A–T)]•poly[d(A–T)]. Similar experiments have been performed on poly[d(G–C)]•poly[d(G–C)] in this study. The pressure dependence of the equilibrium constant for EB binding with poly[d(G–C)]•poly[d(G–C)] was measured at six temperatures ranging from 13.5 to 84.8 °C. The temperature dependence of the deduced molar volume and compressibility changes are shown in Figs. 3 and 4, respectively. Previously published [25] and unpublished data for poly[d(A–T)]•poly[d(A–T)] are shown in Figs. 3 and 4, respectively, for comparison. The value of ΔV for EB binding with poly[d(G–C)]•poly[d(G–C)] becomes more negative with increasing temperature, and the trends are similar for binding with poly[d(A–T)]•poly[d(A–T)] [25]. From 13.5 to 55.8 °C, the value of ΔV decreases with increasing temperature, the average expansivity equals -0.128 ± 0.015 cm^3 mol^{-1} K^{-1} for poly[d(G–C)]•poly[d(G–C)], which is slightly less than the value of -0.154 ± 0.016 cm^3 mol^{-1} K^{-1} reported for the interaction of EB with poly[d(A–T)]•poly[d(A–T)] over a similar temperature range [25]. Higher temperature could be reached for the more thermal stable poly[d(G–C)]•poly[d(G–C)], with the broader temperature range, a slight curvature could be seen with ΔV decreasing faster at temperatures higher than 55.8 °C. If these data are fit with second order polynomial, the slope of the curve reaches -0.22 ± 0.02 cm^3 mol^{-1} K^{-1} at 84.8 °C. Similar trends have been observed for the temperature dependence of compressibility changes from Fig. 4.

In the range from 13 to 55.8 °C, the compressibility change of EB binding to poly[d(G–C)]•poly[d(G–C)] is similar to that of

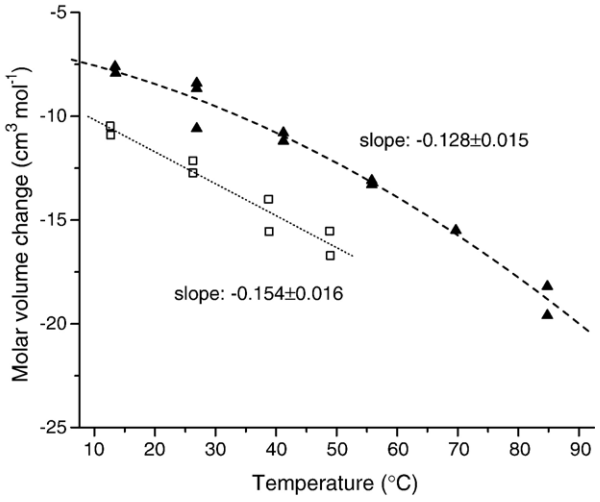

Fig. 3. Temperature dependence of molar volume change of ethidium binding with poly[d(G–C)]•poly[d(G–C)] and poly[d(A–T)]•poly[d(A–T)] in 20 mM Tris–HCl-50 mM NaCl, pH 7.2. The hollow squares are data for poly[d(A–T)]•poly[d(A–T)] [24]. And the solid triangles are data for poly[d(G–C)]•poly[d(G–C)], the slope is an average of slopes between 10 and 60 °C.

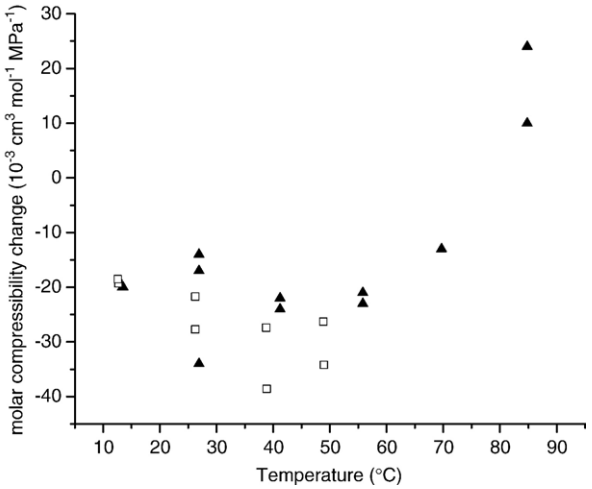

Fig. 4. Temperature dependence of compressibility change of ethidium binding with Poly[d(G–C)]•poly[d(G–C)] and poly[d(A–T)]•poly[d(A–T)] in 20 mM Tris–HCl-50 mM NaCl, pH 7.2. The hollow squares are data for poly[d(A–T)]•poly[d(A–T)] (unpublished data). And the solid triangles are data for poly[d(G–C)]•poly[d(G–C)].

poly[d(A–T)]•poly[d(A–T)]. Binding with either polymer results in negative compressibility changes with the value for binding to poly[d(A–T)]•poly[d(A–T)] being slightly more negative than that for poly[d(G–C)]•poly[d(G–C)]. The compressibility changes are relatively insensitive to temperature for both polymers although at temperatures above ~56 °C the compressibility change of binding with poly[d(G–C)]•poly[d(G–C)] gradually becomes more positive with increasing temperature and changes sign at around 80 °C.

The temperature dependence of K_a for EB binding to poly[d(G–C)]•poly[d(G–C)] is plotted in Fig. 5. By fitting the data with a second order polynomial and assuming a single-step reaction mechanism we found that at 25 °C the enthalpy, equals −7.4± 5.3 kcal mol^{-1}. The large relative error is a consequence of the fact that the enthalpy is calculated from the difference between two large terms each with errors of about 10%. The heat capacity change for binding, ΔC_P, is −121±13 cal mol^{-1} K^{-1} at 25 °C.

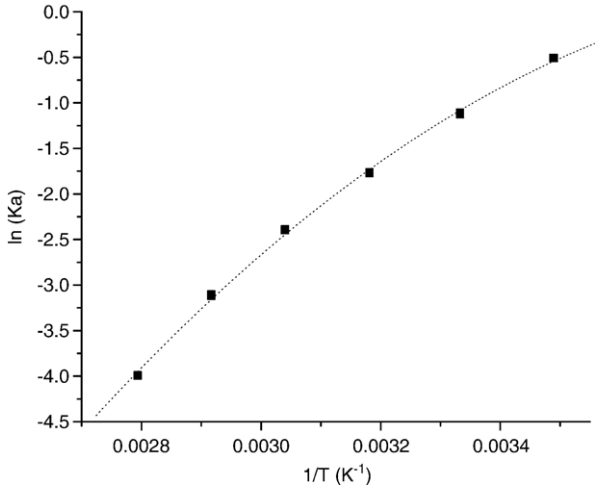

Fig. 5. Temperature dependence of equilibrium constants of ethidium binding with Poly[d(G–C)]•poly[d(G–C)] in 20 mM Tris–HCl-50 mM NaCl, pH 7.2.

4. Discussion

The binding parameters we have obtained agree well with literature results, where they are available [9,16,21,22,26–32,34]. The measured salt dependence of the binding constant (K_a) agrees with the polyelectrolyte theory [35,36] and available literature values [9,22,38]. By analyzing the salt dependence of binding, we deduced the free energy of the different systems at 1 M salt. The resulting free energy, termed ΔG_{other}; eliminates the effect of counter-ion release on binding [36,39]. The values of ΔH in Table 4 are taken from the literature, in all cases they are calorimetrically determined values except in the case of Hoechst 33258, which is a van't Hoff enthalpy. The non-electrostatic component of the entropy change, ΔS_{other}, has been deduced from ΔG_{other} and ΔH. Our volumetric data agree well with literature results where they exist [9–12,27]. We are unaware of other reports on the volumetric properties of daunomycin binding with these three synthetic DNA polymers or for PI binding with poly[d(G–C)]•poly[d(G–C)].

DNA–ligand binding is a complex process with multiple sources of free energy. The major free energy components include conformation free energy, ΔG_{conf}, translational and rotational free energy, ΔG_{r+t}, polyelectrolyte free energy, ΔG_{pe}, and the free energy arising from hydration and molecular interaction, $\Delta G_{hyd\ mol}$. The free energies due to hydration and molecular interaction are considered together because of their close relationship; the formation of a non-covalent complex is almost always associated with desolvation of the interacting molecules. Furthermore, for DNA–ligand interactions, this term will depend on the DNA sequence.

In contrast to this, the other terms, ΔG_{r+t}, and ΔG_{pe}, are independent of the DNA sequence, to a first approximation. Therefore, understanding the thermodynamics of DNA–ligand interactions is contingent on our ability to describe the factors

Table 4
Experimental and literature results*

	ΔV (cm^3/mol)	$\Delta\kappa_T$ (10^{-3} cm^3 mol^{-1} MPa^{-1})	ΔG_{other} (kcal/mol)	ΔH (kcal/mol)	ΔS_{other} (cal mol^{-1} K^{-1})
poly[d(G–C)]•poly[d(G–C)] with					
EB	−10.5	−22	−5.6	−6.3[a]	−2.5
PI	−11.8	−20	−5.5	−7.4[a]	−6.3
DAU	−0.9	−24	−7.4	−8[b]	−2.1
poly(dA)•poly(dT) with					
EB	5.4	−4	−4.3	−1.3[c]	10.1
PI	1.7	−31	−3.6	−1.1[c]	8.3
DAU	15.4	61	−4.8	1.9[b]	22.3
poly[d(A–T)]•poly[d(A–T)] with					
EB	−14.1	−17	−6.1	−9[c]	−9.9
PI	−12.7	−26	−5.9	−6.6[c]	−2.5
DAU	−0.9	23	−7	−5.5[b]	5.0
Hoechst 33258chst 33258	−3.0	−15	−8.1	−6.2[d]	6.3

* The values for ΔV, the compressibility change ($\Delta\kappa_T$), and ΔG_{other} are experimental results. The values for ΔH were taken from the literature (a. [38], b. [62], c. [9], d. [22]). The values for ΔS_{other} were deduced from ΔG_{other} and ΔH.

contributing to $\Delta G_{\text{hyd mol}}$ and ΔG_{conf}. Although it is sequence independent the exact value of ΔG_{r+t}, is still debated [4,40] To compensate for this lack of certainty we have compared the thermodynamic data for similar systems. Assuming that ΔG_{r+t} is the same for all cases, then after correcting for the difference in ΔG_{pe}, which is mostly dependent on the charge of the ligand, the difference in ΔG_{other} compared between different systems provides a good measure of difference in sum of $\Delta G_{\text{hyd mol}}$ and ΔG_{conf}. The latter term, ΔG_{conf}, is relatively non-specific for different intercalators and ΔG_{conf} of minor groove binding is negligible. Thus, differences in $\Delta G_{\text{hyd mol}}$ can be deduced. In the following discussion, we have interpreted the hydration and molecular interaction differences of the systems we have studied on the basis of their differential thermodynamic properties.

4.1. Dissection of the hydration and molecular interactions

We propose that the changes in hydration accompanying the formation of intermolecular complexes consist of three principal components. Each component has a characteristic thermodynamic signature, which can be used to interpret the observed differences in $\Delta G_{\text{hyd mol}}$ and other parameters as the contribution of a single or sum of multiple components.

4.1.1. Burial of non-polar hydrophobic solvent accessible surface, ΔA_{np}

The change in the solvent accessible area of non-polar surface (ΔA_{np}) that occurs as a consequence of ligand binding with DNA has favourable hydrophobic free energy [2,5]. This derives from favourable entropy contributions that accompany the release of hydration water and the loss of unfavourable cavity entropy. This hydrophobic interaction process has been assumed to be equivalent to the transfer of non-polar small molecules between pure liquid and water solution. Near room temperature the enthalpy change of this transfer process is approximately zero [41].

The volume change caused by the formation of a non-covalent complex has two major components: thermal volume change ΔV_{T} and hydration volume change ΔV_{H} [42,43]. Thermal volume is the layer of empty volume generated by solute–solvent vibration. This is a large positive term with strong dependence on solvent accessible molecular surface and not on the properties of the surface. The hydration volume is the change in solvent molar volume due to solute–solvent interaction; it is approximately zero for non-polar surface and negative for polar and charged solute surface [44]. The overall volume change arising from exposing the solute to solvent ranges from large and positive for a non-polar surface to small and positive for polar group to negative for the exposure of a charged group. In the present case, burial of hydrophobic surface results in desolvation and a large negative ΔV, this is dominated by a large negative ΔV_{T}.

In summary, in the case of DNA–ligand binding the signs of ΔG, $-T\Delta S$, and ΔV for Process I are negative and the enthalpy contribution is assumed to be small. When comparing different binding systems, the differences in ΔA_{np}, i.e. $\Delta\Delta A_{\text{np}}$, may be either positive or negative with $\Delta\Delta G$, $-\Delta(T\Delta S)$ and $\Delta\Delta V$ having the same sign as $\Delta\Delta A_{\text{np}}$ and $\Delta\Delta H \sim 0$.

4.1.2. Burial of polar surface and formation of solute–solute H-bonds, ΔAP

The burial of polar surface is associated with the release of water molecules involved in solvating the interacting surfaces and a positive entropy change. On the other hand, there is an enthalpy penalty for dehydration of a polar group that may be offset by a favourable enthalpy for the formation of new interactions between the polar groups of the ligand and DNA. The latter arises mainly from the formation of hydrogen bonds and it is likely to be the dominant term if the solute–solute H-bond is geometrically correct, otherwise H-bond based structures such as DNA duplex will not be formed simultaneously. With negative $-T\Delta S$ and negative ΔH the overall ΔG is also negative and favourable. Chalikian [45] has estimated that for each polar group, ΔG, ΔH and $-T\Delta S$ equal -0.8 ± 0.1 kcal mol^{-1}, -0.33 ± 0.03 kcal mol^{-1} and -0.47 ± 0.09 kcal mol^{-1}, respectively at 298 K. As discussed earlier, burial of a polar group is associated with a negative ΔV with a smaller magnitude than ΔV of burial of non-polar group.

When comparing different binding systems, if the processes are the same in quality and only different in quantity, such as in differences in the amount of polar surface area buried, then the thermodynamic quantities $\Delta\Delta G$, $\Delta\Delta H$, $-\Delta(T\Delta S)$ and $\Delta\Delta V$ will have the same sign as $\Delta\Delta A_{\text{P}}$. If the difference is only in quality, such as in the case of exchanging one kind of polar group with another then, $\Delta\Delta G$, $\Delta\Delta H$ and $-\Delta(T\Delta S)$ are likely to have the same sign, which will be the opposite of that of $\Delta\Delta V$. When the difference is mainly in quantity the sign of $\Delta\Delta V$ is dominated by its thermal volume component; when the difference is only in quality, $\Delta\Delta V$ may be attributed mainly to hydration volume. Intermediate cases may also exist. For example, the buried polar groups may be unable to form a new hydrogen bond or only able to form a weak hydrogen bond in which case ΔG will be less favourable.

4.1.3. Disruption of pattern or structural hydration

DNA possesses large-scale hydration patterns, such as the spine of hydration commonly seen in stretches with a narrow minor groove [46,47]. The highly ordered hydration pattern forms spontaneously and its disruption will have an unfavourable ΔG. With a favourable entropy contribution from release of hydration water, the ΔH is unfavourable and its magnitude is larger than that of $-T\Delta S$ so as to yield an unfavourable ΔG. In other words, this process involves enthalpy–entropy compensation, which is different from Processes I and II. Processes I and II include the first layer of water, while Process III is specifically associated with hydration properties that extend beyond the first layer hydration. For example, strengthening the water–solute interaction by formation of a bridge between two polar groups would have contributions from Process II and Process III. This definition of Processes I and II will facilitate future quantification because all irregular hydration is grouped into Process III. Electrostriction of waters are another form of irregular hydration. In this case there is a partial immobilization of water molecules by DNA phosphate charge and by high charge density pockets in narrow region of DNA minor groove; these interactions also contributes to Process III. However, our

data show that the volumetric properties are relatively insensitive to the salt concentration, the electrostriction effect might not be very significant in this system. To summarize, ΔG, ΔH, and ΔV have the same sign, which is opposite to that of $-T\Delta S$. DNA–ligand binding often involves disruption of DNA hydration pattern and a positive ΔG, ΔH and ΔV for Process III.

Thermodynamic signatures of the three processes

	Process I. Burial of non-polar surface, ΔA_{np}	Process II. Burial of polar surface, ΔA_P	Process III. Disruption of structural water
ΔV	Negative	Negative	Positive
ΔG	Negative	Negative	Positive
ΔH	Negligible	Negative	Positive
$-T\Delta S$	Negative	Negative	Negative

4.2. Analysis of the experimental results

Inspection of Table 4 shows that one can make four general observations regarding the binding of intercalators:

1 The overall affinity and volume change of the binding of the three ligands with the two alternating polymers, poly[d(A–T)]•poly[d(A–T)] and poly[d(G–C)]•poly[d(G–C)], are similar. The binding events are enthalpy driven.
2 The thermodynamic parameters describing binding with poly(dA)•poly(dT) differ significantly from those for binding to the alternating polymers. The binding is weaker, ΔV is more positive, and the interaction is entropy driven.
3 The intercalation of EB and PI are similar aside from the polyelectrolyte factor.
4 Binding of daunomycin has a more positive volume change than EB and PI.

In what follows, we will attempt to rationalize these observations and discuss the small variants besides the general trends.

4.2.1. The similarity of binding with poly[d(A–T)]•poly[d(A–T)] and poly[d(G–C)]•poly[d(G–C)]

From Table 4 one can see that the thermodynamic profiles for intercalation with the alternating sequence DNA polymers are similar; however, the values for the complexes formed with poly(dA)•poly(dT) differ strikingly. With the exception of the complexes formed with poly(dA)•poly(dT), the formation of the non-covalent complexes are enthalpy driven because the favourable entropy contribution from Processes I, II, and III is offset by the loss of translational–rotational entropy associated with a bimolecular reaction, $-T\Delta S_{r+t} \sim 14.9$ (±3.0) kcal/mol [4]. However, there are differences among the systems we have studied.

To compare the sequence dependence of intercalation we need to consider DNA base unstacking. The unstacking of the DNA base pairs is a significant component of what is loosely termed "conformation change" for intercalation. The energetics of the unstacking process depends on the base sequence. It is reasonable to assume that the relative difference between the values for helix–coil transition is a good estimation for the difference in unstacking processes required prior to or concomitant with intercalation. Using the nearest-neighbor approach to study the thermodynamics of DNA, SantaLucia et al., [48], reported that the enthalpies of helix–coil transition at 25 °C are 10.6, 8.4 and 6.4 kcal/mol for GC/CG, AA/TT and AT/TA sequences, respectively; while the free energies are 2.2, 1.0 and 0.7 kcal/mol. If we assume that the enthalpy contribution of the extra hydrogen bond of GC to be roughly 0.9 kcal/mol at 1 M salt [49,50], the above numbers can be modified to be 9.7, 8.4 and 6.4 kcal/mol for enthalpy and 1.3, 1.0 and 0.7 kcal/mol for free energy. The relatively small difference in free energy is a consequence of strong enthalpy–entropy compensation. Similarly, a nearest-neighbor volumetric study [51] showed that the volume changes for helix–coil transitions are 3.6±1.3, −1.6±0.6 and −1.7±0.8 cm^3/mol for GC/CG, AA/TT and AT/TA sequences.

For the three intercalators the difference in binding with G–C and A–T is accounted for by the energetics of the stacking of these sequences (or in this case the energetics of unstacking). For example, in Table 5 the $\Delta\Delta H$ of EB is [ΔH(EB G–C) − ΔH (unstacking of G–C)] − [(ΔH(EB A–T) − ΔH (unstacking of A–T)], where ΔH(EB G–C) and ΔH(EB A–T) are from Table 4 and ΔH (unstacking of G–C) and ΔH (unstacking of A–T) equal to 9.7 and 6.4 kcal/mol, respectively. The values of $\Delta\Delta V$ reported in Table 5 were calculated in the same way as $\Delta\Delta H$. We did not take the sequence dependent unstacking into account for the values we report for the compressibility change.

The analysis summarized in Table 5 shows that there is a strong similarity between binding with poly[d(A–T)]•poly[d(A–T)] and poly[d(G–C)]•poly[d(G–C)]. The thermodynamic parameters for all three ligands show enthalpy–entropy compensation with $\Delta\Delta V$ having the same sign as $\Delta\Delta G_{other}$ and $\Delta\Delta H$. This pattern suggests that the differences arise principally from Process III, disruption of pattern or structural hydration. The enthalpy–entropy compensation arising from disruption of ordered hydration results in a small positive net free energy and a positive volume change due to release of high density hydration water. $\Delta\Delta G_{other}$, $\Delta\Delta H$, and $\Delta\Delta V$ are negative suggesting that the change in the pattern of hydration is more extensive for intercalation with poly[d(A–T)]•poly[d(A–T)] than with poly[d(G–C)]•poly[d(G–C)].

Table 5
Difference between binding with poly[d(G–C)]•poly[d(G–C)] and poly[d(A–T)]•poly[d(A–T)] after calibration of the unstacking conformation change

	$\Delta\Delta H$ (kcal/mol)	$\Delta\Delta G_{other}$ (kcal/mol)	$-\Delta T\Delta S_{other}$ (kcal/mol)	$\Delta\Delta S_{other}$ (cal mol^{-1} K^{-1})	$\Delta\Delta V$ (cm^3/mol)	$\Delta\Delta\kappa_T$ (10^{-3} cm^3 mol^{-1} MPa^{-1})
EB	−0.6	−0.1	0.5	−1.7	−1.7	−5
PI	−4.1	−0.2	3.8	−12.9	−4.4	6
DAU	−5.8	−1	4.8	−16.2	−5.3	−47

ΔΔ corresponds to the value for binding with poly[d(G–C)]•poly[d(G–C)] minus the value for the binding with poly[d(A–T)]•poly[d(A–T)].

This behaviour is also reflected in the similarity of the values of the compressibility and site-exclusion parameter, $n=2$. The temperature dependence of the volume change of the intercalation of EB with poly[d(G–C)]•poly[d(G–C)], -0.128 ± 0.015 cm^3 mol^{-1} K^{-1}, is also similar but slightly more positive than the value for poly[d(A–T)]•poly[d(A–T)] at -0.154 ± 0.016 cm^3 mol^{-1} K^{-1} over a similar temperature range. A more positive value of this parameter can arise from a positive $\Delta\Delta V_T$, a negative $\Delta\Delta V_H$ or a combination of those two. This is in agreement with our analysis, in which we concluded a small negative $\Delta\Delta V$ of hydration pattern change (Table 5) is accompanied by an unstacking process that provides a sizable positive $\Delta\Delta V$ that is dominated by thermal volume.

For PI, the data imply that binding with poly[d(A–T)]•poly[d(A–T)] results in the retention or formation of a more extensive hydration pattern than with poly[d(G–C)]•poly[d(G–C)]. The extra electrostatic charge of PI may be responsible for this; the additional charge may cause a narrowing of the minor groove and help form an extensive hydration pattern. This effect is likely to be more prominent in the AT sequence than GC sequence, hence the observed results. This hypothesis is also consistent with the value of n, the site-exclusion parameter. For poly[d(A–T)]•poly[d(A–T)], $n=3$–4 and $n=2$ for PI intercalation with poly[d(G–C)]•poly[d(G–C)]. The larger value of n may be a consequence of the new hydration structure that effectively extends the binding site.

The thermodynamics of the intercalation of DAU shows a pattern similar to that of PI although the geometry of DAU binding differs significantly from that of EB or PI. Intercalation of EB lengthens the DNA by the length of about one base pair; the side groups of EB likely remain at the new "created" horizontal region and may not significantly disrupt the original DNA hydration pattern unless there are inter-base pair hydration bridges, such as the case of poly(dA)•poly(dT). X-ray crystallographic structures of DAU–DNA complexes show that the sugar ring extends into the minor groove of adjacent base pairs [52–55]; it seems likely that this would disrupt the hydration pattern regardless of the DNA sequence. Since evidence points to poly[d(A–T)]•poly[d(A–T)] being more hydrated than poly[d(G–C)]•poly[d(G–C)], especially in the minor groove [56], the disruption of the more hydrated minor groove hydration of poly[d(A–T)]•poly[d(A–T)] than poly[d(G–C)]•poly[d(G–C)] could account for the observed results for DAU. The compressibility change would also be expected to be greater for the more poorly hydrated poly[d(G–C)]•poly[d(G–C)] than poly[d(A–T)]•poly[d(A–T)]; this corresponds well with the significant compressibility difference observed.

4.2.2. Binding with poly(dA)•poly(dT) is significantly different

The binding to poly(dA)•poly(dT) can be analyzed in a similar manner. The difference between binding with poly(dA)•poly(dT) and poly[d(A–T)]•poly[d(A–T)], after accounting for the base pair unstacking by the methods described above, is given in Table 6. The pattern in Table 6 is typical for Process III. The positive values of $\Delta\Delta G_{other}$, $\Delta\Delta H$, and $\Delta\Delta V$ indicate a stronger disruption in the extensive pattern in poly(dA)•poly(dT) than poly[d(A–T)]•poly[d(A–T)]. The magnitudes of $\Delta\Delta G_{other}$ and $\Delta\Delta V$ in Table 6 are much larger than those reported in Table 5, this may reflect the strength of the extensive hydration pattern of poly(dA)•poly(dT). The results in Table 6 imply that the hydration pattern of poly(dA)•poly(dT) has higher density, higher energy (stronger hydrogen bonds) and lower entropy than that of poly[d(A–T)]•poly[d(A–T)]. This proposition is also supported by the positive differential compressibility observed for EB and DAU. The positive differential compressibility suggests that a more rigid hydration pattern is disrupted upon binding with poly(dA)•poly(dT) than with poly[d(A–T)]•poly[d(A–T)]. The values of the differential compressibility and volume are smaller for PI relative to EB and DAU; this may also be the result of the previously discussed new hydration pattern formed by the extra charge of PI. The minor groove of poly(dA)•poly(dT) is narrower than that of poly[d(A–T)]•poly[d(A–T)]. We propose that the binding of PI to poly(dA)•poly(dT) might lead to a new hydration pattern that is relatively more structured than that arising from a complex between poly[d(A–T)]•poly[d(A–T)] and PI. Thus, the net change in pattern hydration arising from binding of PI will be less for binding to poly(dA)•poly(dT) than for binding with poly[d(A–T)]•poly[d(A–T)].

4.2.3. Binding of EB and PI are similar aside from the polyelectrolyte factor

The difference in binding with PI and EB is summarized in Table 7 with $\Delta\Delta=\Delta(PI)-\Delta\Delta(EB)$; the values of $\Delta(PI)$ and $\Delta(EB)$ are from Table 4. The magnitudes of the values are small. Compared to EB, PI has larger side chain and an additional positive charge. We might speculate about which process contributes more to the differential binding properties of these two molecules; however, the contributions cancel each other out with the magnitude of the difference is small.

We assume that there is no significant difference in burying the side chain of PI with the three DNA polymers. For EB binding we observed consistent values of $d\ln K_a/d\ln[salt]$ ranging from -1.21–-1.29 (Table 2) while we found a large variance for in this parameter for the binding of PI, -2.07, -2.27 and -2.64 for binding with poly[d(G–C)]•poly[d(G–C)],

Table 6
Difference between binding poly(dA)•poly(dT) and poly[d(A–T)]•poly[d(A–T)] after calibration of the unstacking conformation change

	$\Delta\Delta H$ (kcal/mol)	$\Delta\Delta G_{other}$ (kcal/mol)	$-\Delta T\Delta S_{other}$ (kcal/mol)	$\Delta\Delta S_{other}$ (cal mol^{-1} K^{-1})	$\Delta\Delta V$ (cm^3/mol)	$\Delta\Delta\kappa_T$ (10^{-3} cm^3 mol^{-1} MPa^{-1})
EB	5.7	1.5	−4.3	14.3	19.40	13
PI	3.5	2	−1.5	5.1	14.30	−5
DAU	5.4	1.9	−3.5	11.6	16.20	38

$\Delta\Delta$ corresponds to the value for binding with poly(dA)•poly(dT) minus the value for the binding with poly[d(A–T)]•poly[d(A–T)].

Table 7
Difference between binding with PI and EB

	$\Delta\Delta H$ (kcal/mol)	$\Delta\Delta G_{other}$ (kcal/mol)	$-\Delta T\Delta S_{other}$ (kcal/mol)	$\Delta\Delta S_{other}$ (cal mol^{-1} K^{-1})	$\Delta\Delta V$ (cm^3/mol)	$\Delta\Delta\kappa_T$ (10^{-3} cm^3 mol^{-1} MPa^{-1})
poly[d(A–T)]•poly[d(A–T)]	2.4	0.2	−2.2	7.4	1.4	−9
poly(dA)•poly(dT)	0.2	0.7	0.5	−1.8	−3.7	−27
poly[d(G–C)]•poly[d(G–C)]	−1.1	0.1	1.2	−3.8	−1.3	2

ΔΔ corresponds to the value for binding with PI minus the value for the binding with EB.

poly[d(A–T)]•poly[d(A–T)] and poly(dA)•poly(dT), respectively. Aside from experimental error, the larger variance in $d\ln K_a / d\ln[salt]$ for PI binding may be a consequence of the extra charge. The formation of a stronger hydration pattern surrounding the extra charge in a poly(dA)•poly(dT)-PI complex may maximize the impact of the additional charge, leading to the release of more counter-ions.

4.2.4. Binding of daunomycin has a more positive volume change than EB or PI

The singly charged EB was compared with DAU, which has a single positive charge; the comparison is summarized in Table 8 with $\Delta\Delta = \Delta(DAU) - \Delta(EB)$. The values of Δ(DAU) and Δ(EB) are taken from Table 4. The patterns of the thermodynamic parameters given in Table 8 are likely the result of multiple contributions. This is expected with DAU being vastly different from EB in size, number of polar groups, and intercalation direction.

The intercalation of DAU involves the burial of more nonpolar and much more polar surface than EB. The combination of Processes I and II would provide a favourable $\Delta\Delta G_{other,}$ and a negative $\Delta\Delta V$. The fact that $\Delta\Delta V$ is positive may indicate that DAU disrupts the hydration pattern in the minor groove to a greater extent than EB for binding with poly[d(A–T)]•poly[d(A–T)] and poly(dA)•poly(dT), that is, Process III is more unfavourable. With DAU protruding into major groove of DNA, disruption of major groove hydration may make a major contribution to the binding with poly[d(G–C)]•poly[d(G–C)], which has a stronger hydration in its major groove than minor groove [56].

Unlike the phenanthroline ring of EB and PI, the short axis of daunomycinone is parallel to the long axis of base pairs [52,55,57] and may fill the space between the unstacked base pairs less completely. Thus, the positive $\Delta\Delta V$ may be due to the formation of a cavity in the structure. The difference between the binding to the different DNA polymers (Table 8) may arise from differences in Process III as well as differences in quality of ΔA_P, such as an extra H-bond formed by DAU binding with poly[d(G–C)]•poly[d(G–C)].

4.3. Hoechst 33258 binding with poly[d(A–T)]•poly[d(A–T)]

The small negative volume change we measured for this complex, about −3 cm^3 mol^{-1} on average, agrees well with literature data [11]. Hoechst 33258 differs from the intercalators studied in two important ways. First, the flexible ring structures of Hoechst 33258 allow it to fit into the minor groove of AT-rich sequences reasonably well thus avoiding the large conformation change free energy penalty, (~4 kcal/mol) associated with intercalators [58]. The second difference is that Hoechst 33258 is much larger than EB, PI or DAU, thus the binding of Hoechst 33258 is associated with larger reduction in solvent accessible surface and it occupies more base pairs than EB, PI and DAU. The dissection of the free energy by Haq et al. [59] attributed no conformational penalty to the binding of Hoechst 33258. They proposed that the binding free energy arises from a dominant favourable hydrophobic hydration free energy and near-zero free energy arising from the sum of other non-electrostatic, non-covalent interactions, ΔG_{nn}. The favourable hydrophobic free energy is the result of the large reduction in solvent accessible surface, in other words a strong Process I. The insignificant ΔG_{nn} could be the result of cancellation between a favourable Process II and an unfavourable Process III. However, a strong Process I would result in a large negative volume, which is not the case for Hoechst 33258. With the volume change of Process II being small and negative as well, there must be a strong Process III to provide positive volume change to compensate. With Hoechst 33258 binding into minor groove and displacing the hydration pattern for least four base pairs, it is reasonable to assume that Process II plays a very important role. Considering the enthalpy, the magnitude of the ΔH of Process I is small, with counter-ion release is entropy driven, the net ΔH mainly comes from the competition between the favourable ΔH of Process II and unfavourable ΔH of Process III. Unfortunately, there is disagreement in the literature concerning the sign of ΔH of Hoechst 33258 binding. A negative van't Hoff ΔH has been reported for Hoechst 33258 binding with poly[d(A–T)]•poly[d(A–T)] [22] and both positive [59,60] and negative [61] calorimetrically measured

Table 8
Difference between binding with DAU and EB

	$\Delta\Delta H$ (kcal/mol)	$\Delta\Delta G_{other}$ (kcal/mol)	$-\Delta T\Delta S_{other}$ (kcal/mol)	$\Delta\Delta S_{other}$ (cal mol^{-1} K^{-1})	$\Delta\Delta V$ (cm^3/mol)	$\Delta\Delta\kappa_T$ (10^{-3} cm^3 mol^{-1} MPa^{-1})
poly[d(A–T)]•poly[d(A–T)]	3.5	−0.9	−4.4	14.9	13.2	40
poly(dA)•poly(dT)	3.2	−0.5	−3.6	12.2	10	65
poly[d(G–C)]•poly[d(G–C)]	−1.7	−1.8	−0.10	0.4	9.6	−2

ΔΔ corresponds to the value for binding with DAU minus the value for the binding with EB.

ΔH values have been reported for Hoechst 33258 binding with AT-rich oligonucleotides. A positive enthalpy would imply a strong Process III and a negative ΔH would indicate a strong Process II.

In summary, we have proposed that the contribution of hydration to the energetics of DNA–ligand interactions can be described in terms of three principal components. Although casting the data interpretation in these terms facilitates the discussion, it would be interesting and useful to be able to quantify the contribution of each component to the net result. We are currently investigating the possibility of expressing the corresponding volume, free energy, and enthalpy changes of the components in terms of linear combinations of the individual components. If successful this evaluation would have the potential of characterizing DNA–ligand interactions and reveal new quantitative aspects related to the stability of non-covalent complexes through deviations from the standard parameters.

References

[1] R.S. Spolar, J.H. Ha, M.T. Record, Hydrophobic effect in protein folding and other noncovalent processes involving proteins, Proc. Natl. Acad. Sci. U. S. A. 86 (1989) 8382–8385.

[2] J.H. Ha, R.S. Spolar, M.T. Record, Role of the hydrophobic effect in stability of site-specific protein–DNA complexes, J. Mol. Biol. 209 (1989) 801–816.

[3] J.S. Ren, T.C. Jenkins, J.B. Chaires, Energetics of DNA intercalation reactions, Biochemistry 39 (2000) 8439–8447.

[4] R.S. Spolar, M.T. Record, Coupling of local folding to site-specific binding of proteins to DNA, Science 263 (1994) 777–784.

[5] I. Haq, T.C. Jenkins, B.Z. Chowdhry, J.S. Ren, J.B. Chaires, Parsing free energies of drug–DNA interactions, Methods Enzymol. 323 (2000) 373–405.

[6] I. Haq, Part II: the thermodynamics of drug-biopolymer interaction— thermodynamics of drug–DNA interactions, Arch. Biochem. Biophys. 403 (2002) 1–15.

[7] J.B. Chaires, Energetics of drug–DNA interactions, Biopolymers 44 (1998) 201–215.

[8] H.M. Berman, Hydration of DNA— take 2, Curr. Opin. Struct. Biol. 4 (1994) 345–350.

[9] L.A. Marky, R.B. Macgregor, Hydration of dA.dT polymers— role of water in the thermodynamics of ethidium and propidium intercalation, Biochemistry 29 (1990) 4805–4811.

[10] G.Q. Tang, N. Tanaka, S. Kunugi, Effects of pressure on the DNA minor groove binding of Hoechst 33258, Bull. Chem. Soc. Jpn. 71 (1998) 1725–1730.

[11] G.Q. Tang, N. Tanaka, S. Kunugi, Salt effects on fluorescence spectral shifts of DNA-bound Hoechst 33258 and reaction volumes of the minor groove binding, Bull. Chem. Soc. Jpn. 72 (1999) 1129–1137.

[12] F.X. Han, T.V. Chalikian, Hydration changes accompanying nucleic acid intercalation reactions: volumetric characterizations, J. Am. Chem. Soc. 125 (2003) 7219–7229.

[13] D. Rentzeperis, D.W. Kupke, L.A. Marky, Differential hydration of homopurine sequences relative to alternating purine pyrimidine sequences, Biopolymers 32 (1992) 1065–1075.

[14] L.A. Marky, D.W. Kupke, Probing the hydration of the minor groove of A•T synthetic DNA polymers by volume and heat changes, Biochemistry 28 (1989) 9982–9988.

[15] T.V. Chalikian, G.E. Plum, A.P. Sarvazyan, K.J. Breslauer, Influence of drug-binding on DNA hydration— acoustic and densimetric characterizations of netropsin binding to the poly(dAdT)•poly(dAdT) and poly(dA)• poly(dT) duplexes and the poly(dT)•poly(dT)•poly(dT) triplex at 25-Degrees-C, Biochemistry 33 (1994) 8629–8640.

[16] J.L. Bresloff, D.M. Crothers, Equilibrium studies of ethidium–polynucleotide interactions, Biochemistry 20 (1981) 3547–3553.

[17] D. Schmechel, D.M. Crothers, Kinetic and hydrodynamic studies of complex of proflavine with poly A•poly U, Biopolymers 10 (1971) 465–480.

[18] F.M. Pohl, T.M. Jovin, Salt-induced cooperative conformational change of a synthetic DNA— equilibrium and kinetic studies with poly(dGdC), J. Mol. Biol. 67 (1972) 375–396.

[19] J.L. Bresloff, D.M. Crothers, DNA–ethidium reaction-kinetics— demonstration of direct ligand transfer between DNA binding-sites, J. Mol. Biol. 95 (1975) 103–123.

[20] D.J. Patel, L.L. Canuel, Netropsin-poly(dAdT) complex in solution— structure and dynamics of antibiotic-free base pair regions and those centered on bound netropsin, Proc. Natl. Acad. Sci. U. S. A. 74 (1977) 5207–5211.

[21] D. Suh, Y.K. Oh, M.W. Hur, B. Ahn, J.B. Chaires, Daunomycin binding to deoxypolynucleotides with alternating sequences: complete thermodynamic profiles of heterogeneous binding sites, Nucleosides Nucleotides Nucleic Acids 21 (2002) 637–649.

[22] F.G. Loontiens, P. Regenfuss, A. Zechel, L. Dumortier, R.M. Clegg, Binding characteristics of Hoechst-33258 with calf thymus DNA, poly[d (A–T)], and d(CCGGAATTCCGG): multiple stoichiometries and determination of tight-binding with a wide spectrum of site affinities, Biochemistry 29 (1990) 9029–9039.

[23] J.D. McGhee, P.H. von Hippel, Theoretical aspects of DNA–protein interactions— cooperative and non-cooperative binding of large ligands to a one-dimensional homogeneous lattice, J. Mol. Biol. 86 (1974) 469–489.

[24] J.J. Correia, J.B. Chaires, Analysis of drug–DNA binding isotherms: a Monte Carlo approach, MethodS Enzymol. 240 (1994) 593–614.

[25] X.S. Shi, R.B. Macgregor Jr., Temperature dependence of the volumetric parameters of drug binding to poly[d(A–T)]•poly[d(A–T)] and poly(dA)• poly(dT), Biophys. J. 90 (2006) 1729–1738.

[26] W.D. Wilson, Y.H. Wang, C.R. Krishnamoorthy, J.C. Smith, Poly(dT) • Poly(dT) exists in an unusual conformation under physiological conditions— propidium binding to poly(dA)•poly(dT) and poly[d(A–T)]• poly[d(A–T)], Biochemistry 24 (1985) 3991–3999.

[27] R.B. Macgregor, R.M. Clegg, T.M. Jovin, Pressure-jump study of the kinetics of ethidium–bromide binding to DNA, Biochemistry 24 (1985) 5503–5510.

[28] L.E. Xodo, G. Manzini, J. Ruggiero, F. Quadrifoglio, On the interaction of daunomycin with synthetic alternating DNAs— sequence specificity and poly-electrolyte effects on the intercalation equilibrium, Biopolymers 27 (1988) 1839–1857.

[29] J.E. Herrera, J.B. Chaires, A premelting conformational transition in poly (dA) •poly(dT) coupled to daunomycin binding, Biochemistry 28 (1989) 1993–2000.

[30] J.B. Chaires, Biophysical chemistry of the daunomycin–DNA interaction, Biophys. Chem. 35 (1990) 191–202.

[31] J.B. Chaires, Equilibrium studies on the interaction of daunomycin with deoxypolynucleotides, Biochemistry 22 (1983) 4204–4211.

[32] K.J. Breslauer, D.P. Remeta, W.Y. Chou, R. Ferrante, J. Curry, D. Zaunczkowski, J.G. Snyder, L.A. Marky, Enthalpy entropy compensations in drug DNA-binding studies, Proc. Natl. Acad. Sci. U. S. A. 84 (1987) 8922–8926.

[33] S.A. Harris, E. Gavathiotis, M.S. Searle, M. Orozco, C.A. Laughton, Cooperativity in drug–DNA recognition: a molecular dynamics study, J. Am. Chem. Soc. 123 (2001) 12658–12663.

[34] K.E. Rao, J.W. Lown, Molecular recognition between ligands and nucleic-acids— DNA-binding characteristics of analogs of Hoechst 33258 designed to exhibit altered base and sequence recognition, Chem. Res. Toxicol. 4 (1991) 661–669.

[35] G.S. Manning, Molecular theory of polyelectrolyte solutions with applications to electrostatic properties of polynucleotides, Q. Rev. Biophys. 11 (1978) 179–246.

[36] M.T. Record, C.F. Anderson, T.M. Lohman, Thermodynamic analysis of ion effects on binding and conformational equilibria of proteins and nucleic-acids— roles of ion association or release, screening, and ion effects on water activity, Q. Rev. Biophys. 11 (1978) 103–178.

[37] M.T. Record, T.M. Lohman, P. DeHaseth, Ion effects on ligand–nucleic acid interactions, J. Mol. Biol. 107 (1976) 145–158.

[38] W.Y. Chou, L.A. Marky, D. Zaunczkowski, K.J. Breslauer, The thermodynamics of drug–DNA interactions— ethidium–bromide and propidium iodide, J. Biomol. Struct. Dyn. 5 (1987) 345–359.

[39] J.B. Chaires, Dissecting the free energy of drug binding to DNA, Anti-Cancer Drug Des. 11 (1996) 569–580.
[40] I. Luque, E. Freire, Structure-based prediction of binding affinities and molecular design of peptide ligands, Methods Enzymol. 295 (1998) 100–127.
[41] R.L. Baldwin, Temperature-dependence of the hydrophobic interaction in protein folding, Proc. Natl. Acad. Sci. U. S. A. 83 (1986) 8069–8072.
[42] R.A. Pierotti, Scaled particle theory of aqueous and non-aqueous solutions, Chem. Rev. 76 (1976) 717–726.
[43] D.P. Kharakoz, Partial molar volumes of molecules of arbitrary shape and the effect of hydrogen-bonding with water, J. Solution Chem. 21 (1992) 569–595.
[44] T.V. Chalikian, Structural thermodynamics of hydration, J. Phys. Chem. B 105 (2001) 12566–12578.
[45] T.V. Chalikian, Hydrophobic polar groups tendencies of as a major force in molecular recognition, Biopolymers 70 (2003) 492–496.
[46] H.R. Drew, R.E. Dickerson, Structure of a B-DNA dodecamer 3. Geometry of hydration, J. Mol. Biol. 151 (1981) 535–556.
[47] H.C.M. Nelson, J.T. Finch, B.F. Luisi, A. Klug, The structure of an oligo (dA).Oligo(dT) tract and its biological implications, Nature 330 (1987) 221–226.
[48] J. SantaLucia, H.T. Allawi, A. Seneviratne, Improved nearest-neighbor parameters for predicting DNA duplex stability, Biochemistry 35 (1996) 3555–3562.
[49] J. SantaLucia, A unified view of polymer, dumbbell, and oligonucleotide DNA nearest-neighbor thermodynamics, Proc. Natl. Acad. Sci. U. S. A. 95 (1998) 1460–1465.
[50] M.D. Frank-Kamenetskii, Simplification of the empirical relationship between melting temperature of DNA, its GC content and concentration of sodium ions in solution, Biopolymers 10 (1971) 2623–2624.
[51] D.N. Dubins, R.B. Macgregor, Volumetric properties of the formation of double stranded DNA: a nearest-neighbor analysis, Biopolymers 73 (2004) 242–257.
[52] A.H.J. Wang, G. Ughetto, G.J. Quigley, A. Rich, Interactions between an anthracycline antibiotic and DNA— molecular-structure of daunomycin complexed to d(CpGpTpApCpG) at 1.2-Å resolution, Biochemistry 26 (1987) 1152–1163.
[53] C.A. Frederick, L.D. Williams, G. Ughetto, G.A. Vandermarel, J.H. Vanboom, A. Rich, A.H.J. Wang, Structural comparison of anticancer drug DNA complexes— adriamycin and daunomycin, Biochemistry 29 (1990) 2538–2549.
[54] C.M. Nunn, L. Vanmeervelt, S. Zhang, M.H. Moore, O. Kennard, DNA drug-interactions— the crystal-structures of d(TGTACA) and d(TGATCA) complexed with daunomycin, J. Mol. Biol. 222 (1991) 167–177.
[55] M.H. Moore, W.N. Hunter, B.L. Destaintot, O. Kennard, DNA–drug interactions— the crystal-structure of d(CGATCG) complexed with daunomycin, J. Mol. Biol. 206 (1989) 693–705.
[56] T.V. Chalikian, J. Volker, A.R. Srinivasan, W.K. Olson, K.J. Breslauer, The hydration of nucleic acid duplexes as assessed by a combination of volumetric and structural techniques, Biopolymers 50 (1999) 459–471.
[57] S.C. Jain, C. Tsai, H.M. Sobell, Visualization of drug–nucleic acid interactions at atomic resolution. 2. Structure of an ethidium–dinucleoside monophosphate crystalline complex, ethidium- 5-iodocytidylyl (3′–5′) guanosine, J. Mol. Biol. 114 (1977) 317–331.
[58] R.B. Macgregor, R.M. Clegg, T.M. Jovin, Viscosity dependence of ethidium–DNA intercalation kinetics, Biochemistry 26 (1987) 4008–4016.
[59] I. Haq, J.E. Ladbury, B.Z. Chowdhry, T.C. Jenkins, J.B. Chaires, Specific binding Of Hoechst 33258 to the $d(CGCAAATTTGCG)_2$ duplex: calorimetric and spectroscopic studies, J. Mol. Biol. 271 (1997) 244–257.
[60] F.X. Han, N. Taulier, T.V. Chalikian, Association of the minor groove binding drug Hoechst 33258 with $d(CGCGAATTCGCG)_2$: volumetric, calorimetric, and spectroscopic characterizations, Biochemistry 44 (2005) 9785–9794.
[61] J.R. Kiser, R.W. Monk, R.L. Smalls, J.T. Petty, Hydration changes in the association of Hoechst 33258 with DNA, Biochemistry 44 (2005) 16988–16997.
[62] D.P. Remeta, C.P. Mudd, R.L. Berger, K.J. Breslauer, Thermodynamic characterization of daunomycin DNA Interactions— microcalorimetric measurements of daunomycin DNA-binding enthalpies, Biochemistry 30 (1991) 9799–9809.